Domain growth and topological defects in an Ising model with competing interactions

T. Ala-Nissila and J. D. Gunton
Department of Physics, Temple University, Philadelphia, Pennsylvania 19122

K. Kaski
Department of Electrical Engineering, Tampere University of Technology, P.O. Box 527, SF-33101 Tampere 10, Finland
(Received 25 November 1986; revised manuscript received 27 July 1987)

We have studied the kinetics of domain growth in the (4×1) uniaxial [or (2,2)] phase of the two-dimensional anisotropic next-nearest-neighbor Ising (ANNNI) model with Monte Carlo methods using Glauber dynamics. The growth is shown to be spatially anisotropic, with the anisotropy depending strongly on the anisotropy parameter α. In addition to this, a more abrupt change is found as one crosses a wetting transition line in the model. Despite this a dynamical exponent $n \simeq 0.5$ is obtained at low temperatures for all values of α. To explain these results, a phenomenological theory of domain growth developed originally for the clock model is extended to include the uniaxial (4×1) phase. In particular, it is demonstrated that the more abrupt change near the wetting transition occurs due to the disappearance of a vertex-antivertex configuration present in the dry region. Also, the ANNNI model with conserved dynamics is shown to belong to a different universality class than a model with a symmetric $p=4$ phase studied recently.

I. INTRODUCTION

Systems far from equilibrium which undergo a dynamical process of ordering form an important class of problems in nonequilibrium statistical mechanics.[1-3] According to the simplest theoretical models, the growth of domains during the ordering process satisfies a power law of the type

$$\bar{R}(t)\sim t^n, \quad t \geq t_0 \tag{1}$$

where n is the growth exponent and $\bar{R}(t)$ is a quantity measuring the average size of the domains. The quantity t_0 denotes an initial transient time after which (1) is satisfied. Another important quantity in characterizing the growth is the nonequilibrium structure factor $S(\mathbf{k},t)$ which in almost all cases studied so far, satisfies the time-dependent scaling relation

$$S(k,t)=\bar{R}^{\,d}(t)F(k\bar{R}(t)), \quad t \geq t_0 \tag{2}$$

where d is the dimensionality and F is a scaling function. The growth law (1) and the scaling property (2) indicate that the system has a characteristic time-dependent length and that the domain growth is self-similar. Following ideas developed for static critical phenomena, it has been proposed that there exist *dynamical universality classes*. These would be characterized in the simplest case by a dynamical exponent, and possibly also a universal form of the scaling function $F(x)$. The universality classes would mainly be determined by a few key features of the system, including the ground-state degeneracy p and the conservation laws for the system, including the order parameter Ψ. At the moment perhaps the only universality class which has been firmly established[2-10] is that of the nonconserved $p=2$ Ising system with $n=\frac{1}{2}$ for which derivations of the scaling function also exist.[6-8] In general, we have, at best, an incomplete understanding of these universality classes at the present time. Recent studies suggest[9-18] that additional features, such as topological defects and uniaxiality of the ground state may play a role in determining the dynamical behavior, and possibly universality. From a theoretical point of view, a satisfactory determination of the universality classes requires proper identification of the underlying physical processes determining universal behavior. This is largely missing, except for the curvature driven $p=2$ Ising case mentioned above.

An additional interesting feature in the dynamics of domain growth is the occurrence of a wetting or an interfacial adsorption transition.[19] These phase transitions occur in a large class of lattice gas models, and in particular for $(p\times 1)$ uniaxial phases with $p \geq 3$.[20-23] They involve transitions between different types of domain walls, and are thus expected to have some influence on the domain growth, during which several types of walls can exist. In our previous study[16] in which the effects of a wetting transition were briefly studied for the uniaxial (2,2) phase with a conserved density, rather nontrivial results were obtained. We will discuss these and more recent results later in some detail.

In this paper we will determine the effects of a wetting transition on the kinetics of domain growth in the $p=4$ phase of the two-dimensional anisotropic or axial next-nearest-neighbor Ising (ANNNI) model[24-27] with Glauber dynamics. We will also discuss both our previous[15,16] and some new results for the conserved density case and the common features shared by the Glauber and Kawasaki models. To begin with, the Hamiltonian for this model in spin representation is

$$H=-\sum_{\langle ij\rangle}\left(J_1 s_{ij}s_{i+1,j}-J_2 s_{ij}s_{i+2,j}+J_0 s_{ij}s_{i,j+1}\right), \tag{3}$$

where $J_i > 0$, $i = 0, 1, 2$, and the summation goes over all sites of a square lattice with Ising spins $s_{ij} = \pm 1$. The indices i and j correspond to the x and y directions, respectively. Equation (3) can be transformed into lattice-gas form by using the change of variables $c_{ij} = (1 + s_{ij})/2$, where the quantities c_{ij} are either 0 or 1, corresponding to empty and occupied sites, respectively. In this form the Hamiltonian becomes[16]

$$H - \mu N_t = - \sum_{\langle ij \rangle} (\phi_1 c_{ij} c_{i+1,j} - \phi_2 c_{ij} c_{i+2,j} + \phi_0 c_{ij} c_{i,j+1}) \tag{4}$$

with $\phi_i = 4J_i$, $i = 0, 1, 2$. The chemical potential is $\mu = \phi_1 - \phi_2 + \phi_0$, and the total lattice density is $N_t = N_\rho$. A modified form of the ANNNI model in an external field with $J_1 < 0$ has been extensively studied as a model of O/Pd(110).[14,21,23,28] [This system has a (3×1) uniaxial phase.] In Fig. 1 we show the phase diagram of the ANNNI model obtained by using the standard parametrization[24] $\alpha = J_2/J_0$ and $J_1 = (1 - \alpha)J_0$. Figure 1 exhibits the three different ordered phases in the model: an incommensurate (I) phase, a commensurate ferromagnetic (F) phase, and a modulated (2,2) antiphase. Based on well-known theoretical arguments,[2,3] it is clear that the domain growth in the *ferromagnetic* phase must belong to the $p = 2$ universality class. However, the (2,2) antiphase is a uniaxial (4×1) phase with a higher ground-state degeneracy $p = 4$. It consists of an alternating sequence of two ferromagnetic layers of up and down spins in the x direction, as shown schematically in Fig. 1. For this ground state, the relevant order parameter has two components[26]

$$\psi_\alpha = (1/NM)^{1/2} \sum_{n,m} s_{nm} \exp[i(\mathbf{Q}_\alpha \cdot \mathbf{r}_{nm})], \quad \alpha = 1, 2 \tag{5}$$

where $\mathbf{Q}_1 = (2\pi/a)(\frac{1}{4}, 0)$ and $\mathbf{Q}_2 = (2\pi/a)(-\frac{1}{4}, 0)$ are the two positions of the Bragg peaks and N and M are the number of sites in the x and y directions, respectively. Due to the high degeneracy of the (2,2) antiphase, a nontrivial wetting transition occurs which divides the phase diagram into a dry and a wet region. The position of this line is indicated by the dashed line in Fig. 1. This wetting transition takes place when a soft superheavy (superlight) wall decays to three heavy (light) walls. Symbolically, $A \mid D \rightarrow A \mid B \mid C \mid D$, i.e., the two phases B and C "wet" A and D (see Fig. 2). The properties of this wetting transition have been studied in detail.[22,23] At $T = 0$, the wetting occurs at $\alpha = \frac{1}{2}$. We note that the parametrization used here has the advantage that $\alpha = 1$ is a special *decoupling point* in which the ANNNI model becomes equivalent to two uncoupled layered antiferromagnetic Ising models.[26] Consequently, there is no nontrivial wetting transition at $\alpha = 1$; also the melting point is exactly known at this point.

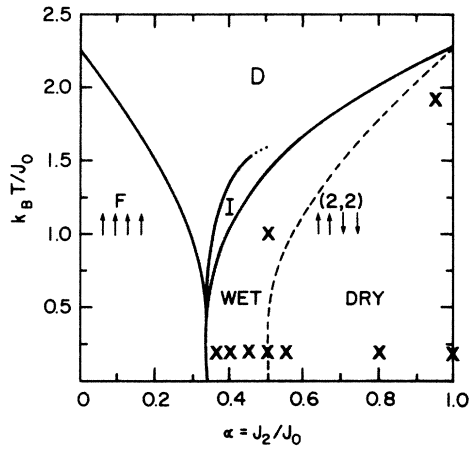

FIG. 1. Schematic phase diagram of the two-dimensional ANNNI model showing the disordered (D) phase, the commensurate (2.2), ferromagnetic (F), and the incommensurate (I) phase. The F-D line is from Ref. 35, and the (2.2)-I line from Ref. 37. (Note that Ref. 32 has a new estimate for the latter which is slightly below the result shown here.) The dashed line denotes the approximate position of the wetting line within the (2.2) antiphase (Ref. 32). The crosses depict the values of $k_B T_f/J_0$ for which the quenches with Glauber dynamics were performed.

In this paper we employ a comprehensive Monte Carlo study to determine the dynamical growth exponent n for the ANNNI model. We find $n \simeq 0.5$ holds to a good degree of accuracy at low temperatures everywhere within the (2,2) phase. Also, the growth proceeds anisotropically between the x and y directions, and generalized anisotropic scaling is found to hold to a good degree of accuracy. However, we find an abrupt change in this anisotropic growth mode as the wetting transition takes place. Namely, everywhere in the dry region the x direction grows faster than the y direction, but immediately after wetting the opposite occurs. To explain these rather unexpected results, we invoke theoretical arguments developed originally by Kawasaki[11,12] for the p-state clock model ($p \geq 3$) and extend these to include the uniaxial (4×1) phase. In particular, both the universal growth exponent $n = \frac{1}{2}$ and the sudden *nonuniversal* change in the anisotropic growth mode can be explained by the existence of a vertex-antivertex configuration which becomes unfavorable due to the wetting transition. This demonstrates the striking effect of a wetting transition on the growth of domains in a system with uniaxiality. Since phases of this type are often encountered in physisorbed and chemisorbed systems, such as for example in O/Pd(110), we expect our results to have relevance in corresponding experiments where phenomena of the type we describe here may be observed.[14] From another point of view, we also expect our results to have some relevance in clarifying the physical mechanisms behind the dynamical universality classes. Namely, in an earlier study[16] we have also found that the ANNNI model with conserved (Kawasaki) dynamics has a growth exponent $n \simeq 0.5$ (at least in the dry region) in contrast to an earlier work by Sadiq and Binder[13] who suggested $n = \frac{1}{3}$ in a model with a *symmetric* $p = 4$ phase. As discussed later, we believe this to be an indication of different physical growth mechanisms in these two models, and possibly to signify that uniaxiality is a

relevant parameter in determining the dynamical universality classes.

II. MONTE CARLO RESULTS FOR THE GLAUBER MODEL

We have studied the kinetics of the domain growth in the ANNNI model by quenching instantaneously from a high-temperature ($k_BT/J_0=\infty$) disordered phase to several temperatures, as well as for various values of α below the phase-transition line of the (2,2) antiphase. These points for the Glauber "spin-flip" dynamics are indicated in Fig. 1 with crosses. For an adsorbate system, these dynamics would correspond to random adsorption and desorption events, which occur with a constant rate. Square lattices of sizes 120×60, 128×128, 100×200, 128×140, and 140×140 were used, with fully periodic boundary conditions to study the effects of finite size. Usually we have performed a minimum of 400 quenches for each system to obtain reliable ensemble averages and compensate for the lack of "self-averaging" far from equilibrium[29] which was evident during our simulations. Also, in order to avoid spurious percolation effects, time sampling of the data was stopped when $\bar{R}(t)$ became about one-fifth of the maximum possible value (i.e., the linear size of the system). Our results have very good statistics and show no systematic finite-size effects.

A. Dynamical behavior of the domain walls and excitations

After the system is quenched to an unstable low-temperature state, domains form as the symmetry of the order parameter is broken and grow in time. This growth far from equilibrium occurs via a competition between the randomly chosen degenerate ground-state phases A, B, C, and D. In Fig. 2 we depict all the energetically different domain walls possible in the (2,2) antiphase.[16] During the growth all of these are in principle present, although the energetically most favorable ones are expected to dominate at late times. There are also defects present for which the "phase-shift" condition is not fulfilled. In Fig. 2 we show two of the most important types of excitations encountered in the system, namely lattice defects and "soft heavy-light" excitations. We have followed the statistics and the role of all these distinct domain walls and excitations in detail during growth. Besides yielding detailed information about the behavior of the system, this data can also be used to define a measure of length separately for the x and y directions.[15,16] Namely, effective domain areas $A_x(t)$ and $A_y(t)$ for the two axial directions can be defined through

$$\bar{R}_i^2(t)\propto A_i(t)\propto[N_i(t)-N_i(\infty)]^{-2},\quad i=x,y \tag{6}$$

where $N_i(t)$ is the number of domain walls at time t and $N_i(\infty)$ is the equilibrium value of N_i at a given temperature for a given value of α. This definition is less sensitive to the choice of $N_i(\infty)$ than that obtained by computing the excess energy ΔE, and also gives information about the anisotropy of the growth between the two axial directions.

1. Growth in the dry region

In Fig. 3 we show a series of typical domain configurations for the ANNNI model at the decoupling point $\alpha=1$. Typically, the growth of domains is quite rapid, as in the $p=2$ nonconserved case.[10] It is evident from these figures that two types of walls, the heavy-light ($A\,|\,B$) and soft superheavy-light ($A\,|\,D$) walls dominate the configurations after an initial transient time. In addition, an anisotropy in the domain growth is clearly visible. The domains percolate more rapidly in the x direction than in the y direction, which indicates an anisotropic growth mode. In Figs. 4(a) and 4(b) we depict both the absolute and relative amounts of walls and excitations as a function of time for $\alpha=1$ and $k_BT/J_0=0.2$ for a 128×128 system. These figures confirm our observation that after a short transient time only the $A\,|\,D$ and $A\,|\,B$ walls are present in the sys-

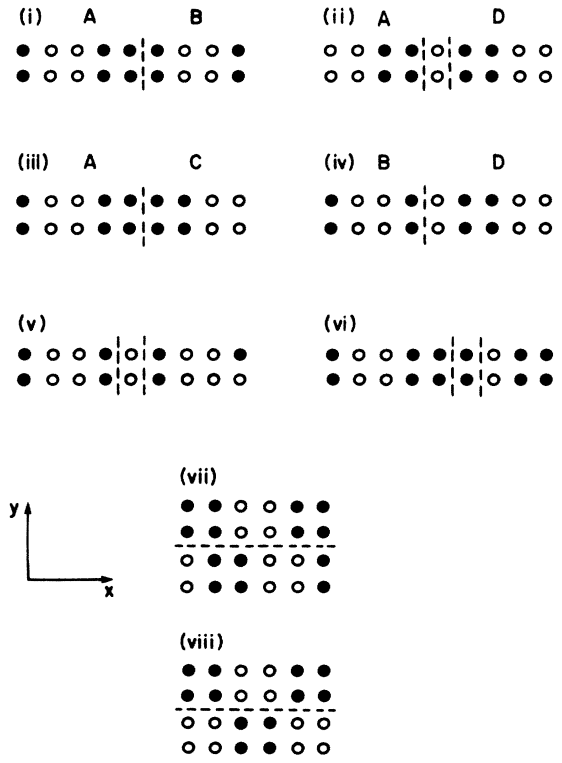

FIG. 2. All the energetically different types of domain walls in the ANNNI model which have been followed during the growth: (i) heavy-light (wet $A\,|\,B$) wall, (ii) soft superheavy-light (dry $A\,|\,D$) wall, (iii) superheavy-light wall, and (iv) medium wall. (v) and (vi) indicate the two most important low-energy excitations encountered in the configurations, the soft heavy-light excitations and the lattice defects, respectively. Excitations consisting of combinations of some of these domain walls and defects are also encountered during domain growth. (vii) and (viii) show the two possible antiphase boundaries in the y direction, of which (vii) is energetically more favorable.

tem. They occur in equal amounts within the accuracy of our results. This is another indication that the solid-on-solid calculation, which was performed in an earlier study[22] of the wetting transition, correctly predicts a degeneracy of the two free energies $\sigma_{A|B}$ and $\sigma_{A|D}$ at this special point.

As α becomes less than one, the degeneracy of the two walls is broken. The $A|B$ walls become energetically more favorable than the single $A|D$ walls and a suppression of the latter should occur. To study this quantitatively, we have followed the domain growth at the same low temperature as before ($k_BT/J_0=0.2$) for

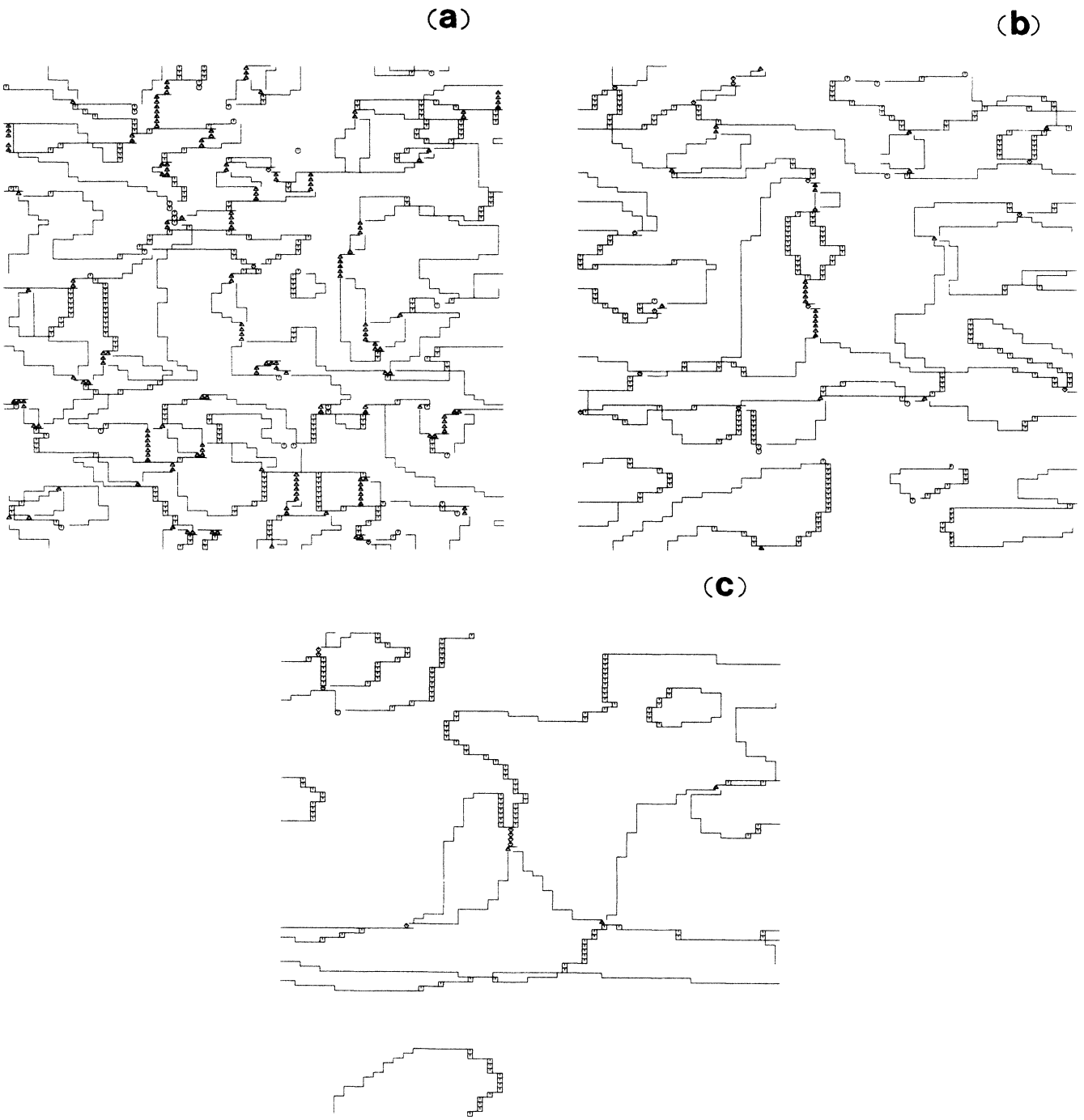

FIG. 3. Figures of typical configurations for a 100^2 system at the decoupling point $\alpha=1.0$, $k_BT_f/J_0=0.2$: (a) 10 Monte Carlo steps (MCS)/site, (b) 20 MCS/site, and (c) 60 MCS/site. At this special point there is an exact degeneracy between the heavy-light and soft superheavy-light walls which are depicted by straight lines and squares, respectively. Other types of walls and excitations are also shown: triangles correspond to superheavy-light walls, diamonds to medium walls, crosses to heavy-light excitations, and circles to lattice defects.

the two values of $\alpha=0.8$ and $\alpha=0.55$. In Figs 4(c) and 4(d) we display the statistics of domain walls for a 140×140 system at $\alpha=0.8$. As expected, a suppression of the soft superheavy-light walls is encountered. We have also studied the 128×128 system very close to the wetting line at $\alpha=0.55$. The results in this case are very similar to the previous statistics, except that a further reduction of the $A \mid D$ walls is seen.

We have not tried to perform a systematic study of the temperature dependence of growth in the dry region, since the theory in this case is not completely understood. Instead, in order to qualitatively see the effect of a high temperature we have quenched a 140×140 system at $\alpha=0.9$ to $k_BT/J_0=1.9$ which is a point very close to the commensurate-incommensurate transition line of the ANNNI model. In Fig. 5 we display snapshots of typical configurations (for a smaller system) encountered at this high temperature. The domain

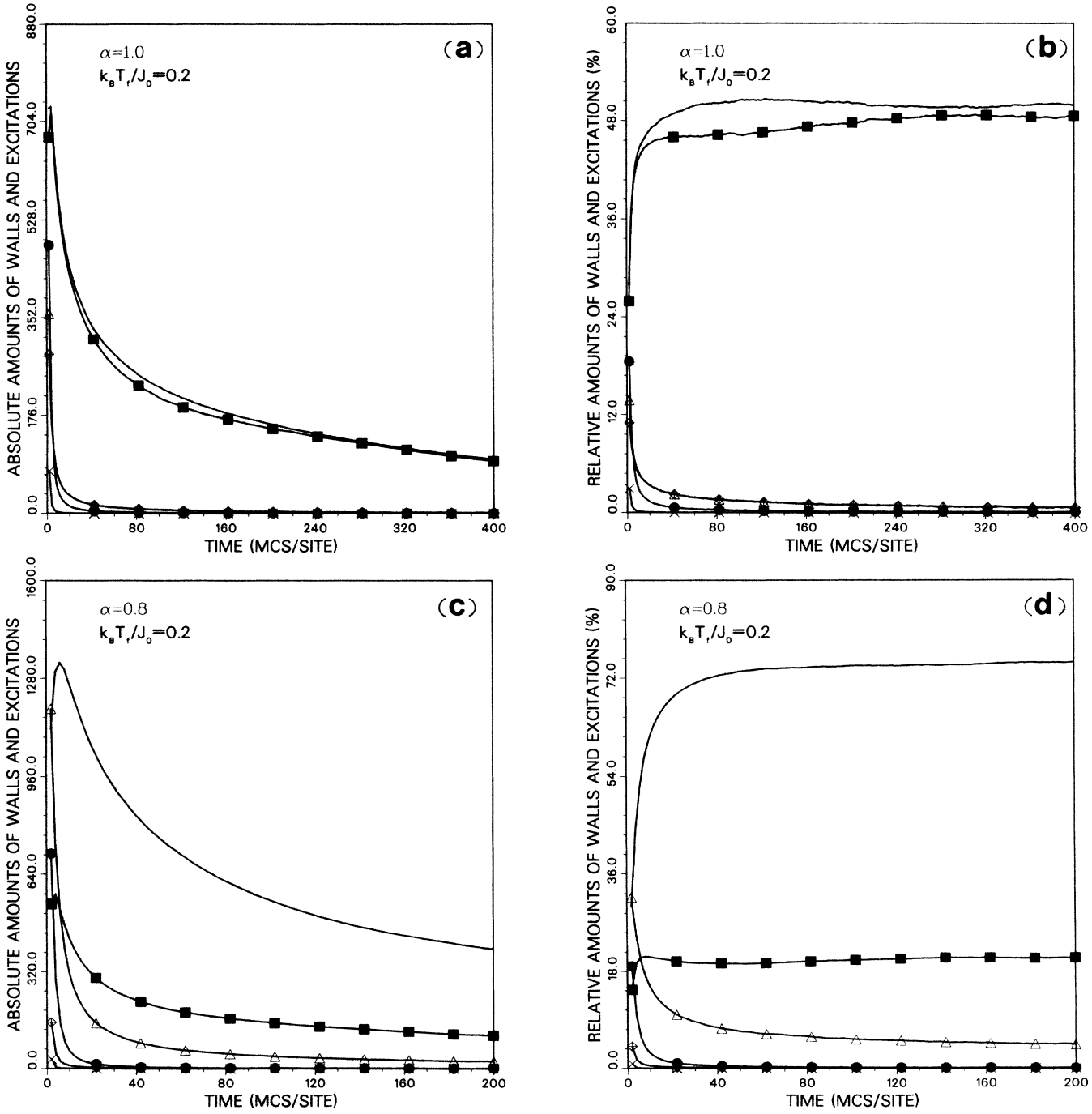

FIG. 4. Statistics of domain walls and excitations for the kinetic ANNNI Glauber model in the dry region of the phase diagram: (a) absolute and (b) relative amounts of walls and excitations at the decoupling point $\alpha=1.0$, $k_BT/J_0=0.2$ for a 128^2 system; (c) absolute and (d) relative amounts of walls and excitations for $\alpha=0.8$, $k_BT_f/J_0=0.2$ in the case of a 140^2 system.

growth seems to proceed in a similar fashion as at lower temperatures, except that a very large number of defects appear in the system. These defects are now thermally generated and seem to persist throughout the growth. Their amount seems to equilibrate to a constant value of about 2.4% of the number of total lattice sites. Also, they seem to break down the domain boundaries to some extent and make them effectively rough. We have also determined the domain-wall statistics for a 140×140 system. The number of lattice defects is very large and almost independent of time. We expect the presence of these excitations and the domain-wall roughness to have

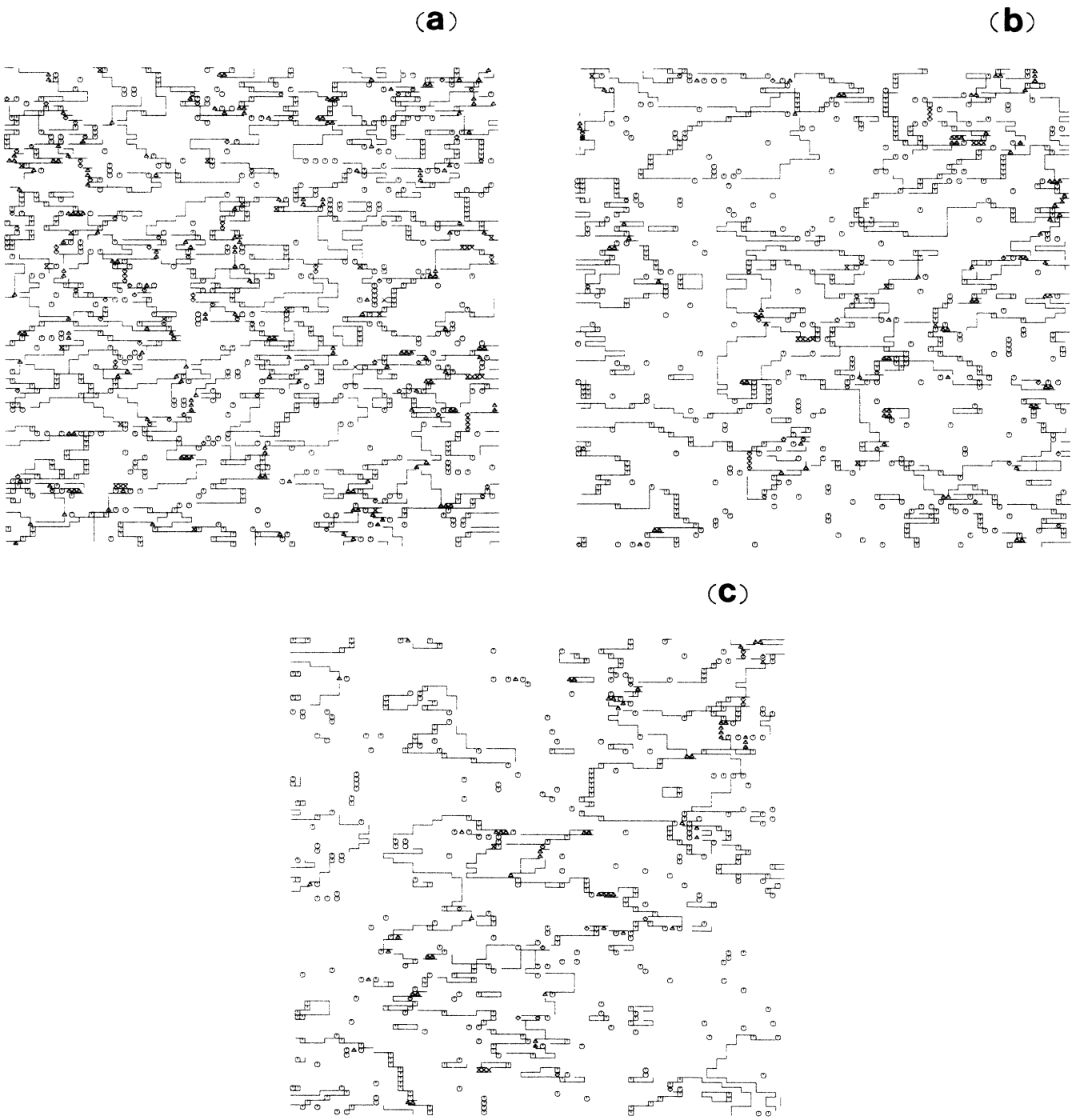

FIG. 5. Some of the typical configurations for a 100^2 system at a high temperature with $\alpha=0.9$, $k_BT_f/J_0=1.9$: (a) 10 MCS/site, (b) 40 MCS/site, and (c) 100 MCS/site. Symbols correspond to those in Fig. 3.

some effect on the growth law, as we will later discuss. As far as other excitations are concerned, their amounts remain below 10% even at these high temperatures.

2. *Growth in the wet region*

When the anisotropy parameter α becomes less than $\frac{1}{2}$ (at $T=0$), the system undergoes a wetting transition as discussed above. This is expected to take place during the early stages of the domain formation, where soft superheavy-light or dry walls decay to heavy-light or wet walls. This change, in the nature of the domain walls in the system, is expected to affect the growth law. In Fig. 6 we show a typical set of domain configurations at $\alpha=0.5$, $k_BT/J_0=0.2$, which is in the immediate vicinity of the wetting line. As expected, practically all dry

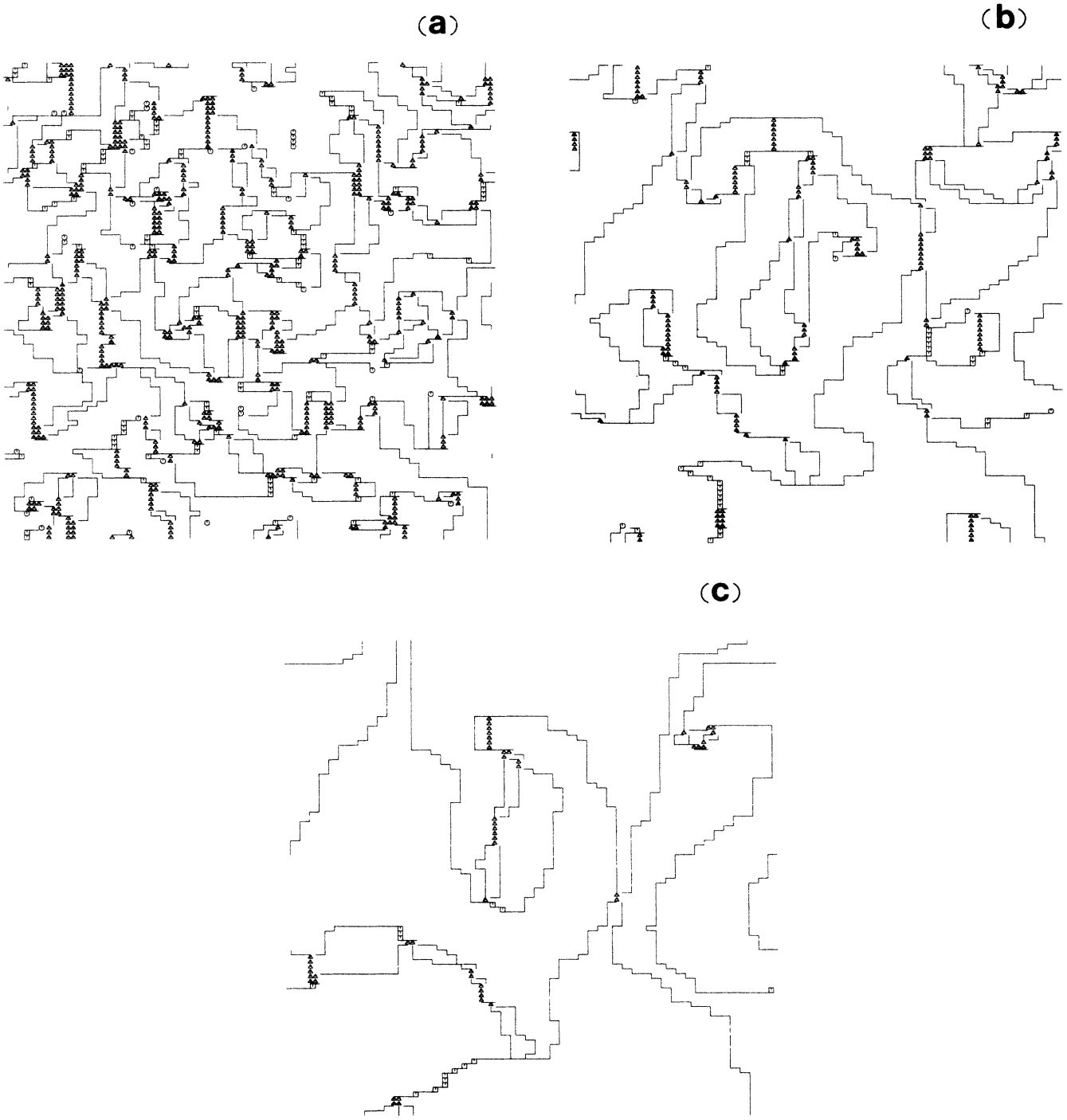

FIG. 6. Time evolution of domains for a 100^2 wet system in the immediate vicinity of the wetting line ($\alpha=0.5$, $k_BT_f/J_0=0.2$): (a) 10 MCS/site, (b) 40 MCS/site, and (c) 100 MCS/site. The dry soft superheavy-light walls have now disappeared almost completely, but seem to persist at the vertex junctions. A change in the anisotropic growth mode is clearly visible in these figures.

walls have disappeared from the system. There is also an apparent change in the anisotropic growth mode. The growth seems to proceed more quickly in the y direction, which is opposite to what was observed in the dry region. In Figs. 7(a) and 7(b) we depict the statistics of domain walls and excitations for a 140×140 system at $\alpha=0.5$, $k_BT/J_0=0.2$. The effect of the wetting transition is now evident in the lack of dry walls at later times.

To follow the behavior of the domain walls as α decreases towards $\frac{1}{3}$, we have quenched systems at low temperature $k_BT/J_0=0.2$ for $\alpha=0.45$, 0.4, and 0.35. In Figs. 7(c) and 7(d) we show the statistics of walls and excitations for a 128×128 system at $\alpha=0.45$. There is a strong increase in the number of superheavy-light walls which eventually disappear from the systems. The result

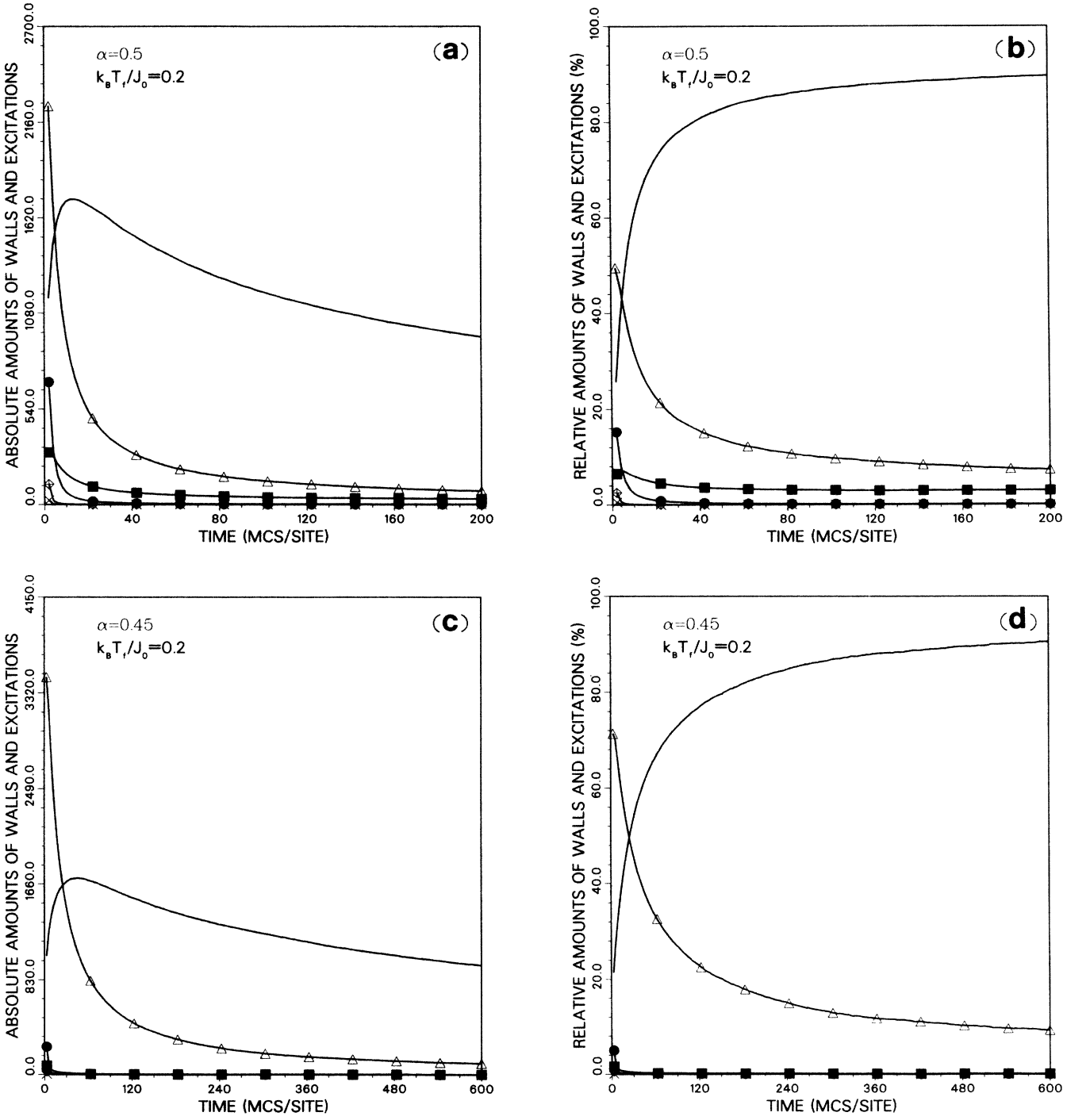

FIG. 7. Statistics of domain walls and excitations for the kinetic ANNNI Glauber model in the wet region of the phase diagram: (a) absolute and (b) relative amounts of domain walls and excitations for a 140^2 system at $\alpha=0.5$, $k_BT_f/J_0=0.2$; (c) absolute and (d) relative amounts of walls and excitations for a 128^2 system at $\alpha=0.45$, $k_BT_f/J_0=0.2$.

of this is a slowing down effect, especially in the x direction where these walls exist. This is clearly seen in the figures of the domain-wall statistics. Similar results are found at $\alpha=0.4$. Finally, we have quenched a 128×140 system very close to the ferromagnetic phase boundary at $\alpha=0.35$, $k_BT/J_0=0.2$. In Fig. 8 we show a series of snapshots of configurations encountered in a smaller system in this case. The number of heavy-light clusters is very large, and there is a strong slowing down effect. We have also studied the domain wall statistics for the large system. There is an overwhelming abundance of heavy-light clusters as we have predicted, but at very

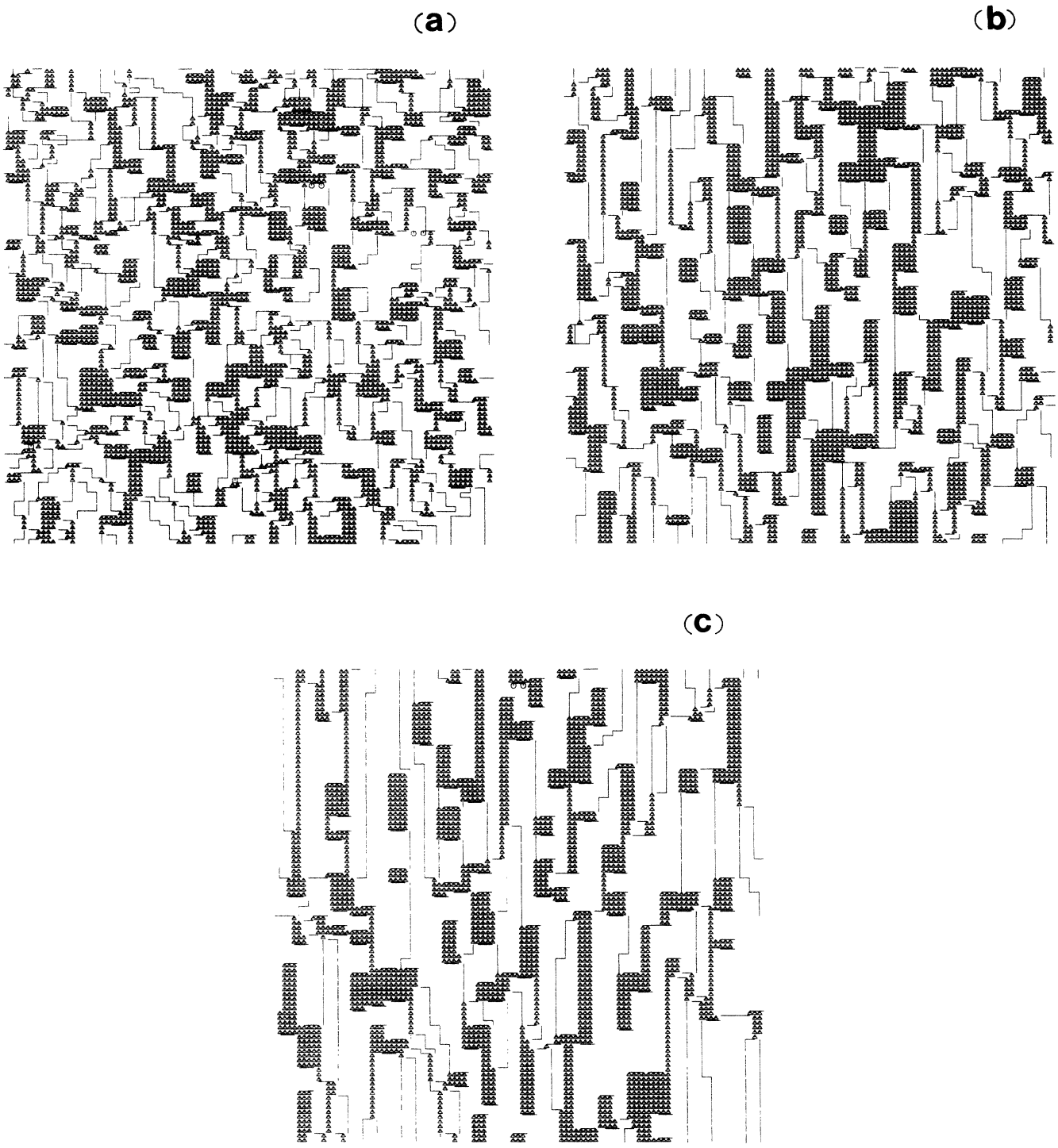

FIG. 8. Series of typical domain configurations for a 100^2 system close to the (2,2)-incommensurate phase boundary at $\alpha=0.35$, $k_BT_f/J_0=0.2$: (a) 10 MCS/ site, (b) 100 MCS/site, and (c) 500 MCS/site. Again, the symbols correspond to Fig. 3. There is a dramatic slowing-down effect caused by the appearance of heavy-light clusters (denoted by triangles) in the system. Also, the anisotropy of the domains is very pronounced.

late times the system still equilibrates.

An interesting feature of the statistics of walls mentioned above is that the number of superheavy-light $A \mid C$ walls has increased strongly. Far from equilibrium these walls which must decay to heavy-light walls at finite temperatures, can obviously be present and should indeed become more common as α is decreased towards $\frac{1}{3}$. Namely, as was mentioned in an earlier study[22] of the wetting transition, in addition to the $A \mid D \rightarrow A \mid B \mid C \mid D$ equilibrium wetting transition, there is a competing transition which occurs only at the point $T=0$, $\alpha=\frac{1}{2}$. In this transition, one heavy-light and one superheavy-light wall emerge, i.e., $A \mid D \rightarrow A \mid C \mid D$. At low temperatures this will still compete with the equilibrium transition, and far from equilibrium the resulting $A \mid C$ walls will exist for a finite time. Indeed, at zero temperature there exists an infinite but countable sequence of wetting transitions of this type, which are of "higher order" in the sense that they do not persist for $T>0$. Namely, the phase-shift condition can be fulfilled in several different ways. In the most general case this can be done by introducing $(2n-1)$ $A \mid C$ walls and $(3m-2)$ $A \mid B$ walls between the dry A and D phases, where m and n are arbitrary positive integers. The sequence of points where these transitions take place is given by the condition

$$\sigma_{A \mid D}=(2n-1)\sigma_{A \mid C}+(3m-2)\sigma_{A \mid B} . \tag{7}$$

Inserting the corresponding values from Ref. 22 gives

$$\alpha=(3m+4n-3)/(9m+12n-13), \quad m,n=1,2,3,\ldots . \tag{8}$$

For $m=n=1$, the simple $A \mid D \rightarrow A \mid C \mid D$ transition point at $\alpha=\frac{1}{2}$ is recovered. Also, for either m or n fixed the phase-boundary point $\alpha=\frac{1}{3}$ is exactly obtained when the infinite limit is taken for the variable which is not fixed. In the case $m=1$ and for increasing n the sequence of transition points goes as $\{\frac{1}{2}, \frac{2}{5}=0.4, \frac{3}{8}=0.375, \frac{4}{11}\simeq 0.364, \frac{5}{14}\simeq 0.357, \ldots\}$. On the other hand, for $n=1$ and increasing m the corresponding set is $\{\frac{1}{2}, \frac{7}{17}\simeq 0.412, \frac{5}{13}\simeq 0.385, \frac{13}{35}\simeq 0.371, \frac{4}{11}\simeq 0.364, \ldots\}$. Another way of satisfying the phase-shift condition is to introduce $n(2m+1)$ AB walls, where again n and m are positive integers. This condition gives only one new sequence which goes as $\{\frac{1}{2}, \frac{3}{7}\simeq 0.429, \frac{2}{5}=0.4, \frac{5}{13}\simeq 0.385, \frac{3}{8}\simeq 0.375, \ldots\}$ for $n=1$ and m increasing. Although these transitions do not persist at finite temperatures in equilibrium, they offer an alternative route to the formation of large clusters of adatoms or vacancies as α is reduced. Of course, this argument is just a way of pointing out that an increased stability of heavy-light clusters is really expected as one approaches $\alpha \rightarrow \frac{1}{3}^{+}$.

Similarly, to the dry region we have performed only one quench at high temperatures in the wet region. This was done at the point where $\alpha=0.5$, $k_B T/J_0=1.0$, for a 128×128 system. The results are very similar to lower temperatures, Figs. 7(a) and 7(b). There is, however, a slight increase in the number of lattice defects, as well as some additional domain-wall roughness in the configurations.

B. The growth law

In order to reliably analyze the underlying growth law of the domains we have studied the behavior of several definitions for the characteristic length $\bar{R}(t)$. A measure of the long-range correlations in the system can be obtained by using the anisotropic (unnormalized) structure factor $S(\mathbf{k},t)$ which is defined as

$$S_\alpha(\mathbf{k},t)=\left\langle \left| \sum_{n,m} s_{nm} \exp\{i[(\mathbf{Q}_\alpha+\mathbf{k})\cdot \mathbf{r}_{nm}]\} \right|^2 \right\rangle , \quad \alpha=1,2 \tag{9}$$

where $\mathbf{k}$ is the deviation from the Bragg positions. Here we limit ourselves to the case $k_x, k_y \geq 0$ for which we compute $S(\mathbf{k},t)$ as discussed later. The peak of this structure function $S(0,t)$ defines a length via[13]

$$\bar{R}(t)^2=S(0,t)/\Psi_T^2 . \tag{10}$$

Here Ψ_T denotes the equilibrium value of the order parameter. At low temperatures, such as at $k_B T_f/J_0=0.2$ which we have mainly studied, it is expected that $\Psi_T \simeq 1$. In other words, fluctuations in long-range order should be very small at low T. At higher temperatures this is not necessarily true. However, we have not tried to estimate Ψ_T for high values of T. The other measures of length we have used are the effective domain areas defined in Eq. (6). For this case we have also set $N_i(\infty)\equiv 0$.

To test the underlying growth law we have assumed that it can be described with a simple power law of the form (1). We have performed standard numerical least-squares fitting of our data to the expression

$$y(t)-y(t_0)=D_i(t-t_0)^{2n_i}, \quad i=x,y \tag{11}$$

where $y(t)\equiv \bar{R}_i^2(t)$. There are two main reasons for using this type of fitting procedure. First, we expect an initial transient time t_0 to be present in the system before the actual universal growth law takes over. Second, (11) is less sensitive to the (nonuniversal) initial part of the data than logarithmic fitting functions, which are often used to obtain an estimate for n.

In Table I we show the results of our fitting to $S(0,t)$ for all the quenches performed in the dry and wet regions. At low temperatures the results clearly indicate an average exponent of $2n\simeq 1.0$ *independent* of the anisotropy parameter α. Even very close to the ferromagnetic boundary this result holds to a very good degree of accuracy. This is a strong indication that a universal growth mechanism governs the system and that the growth law is very well described by a simple power law of the type (1). From Table I it is also evident that the average, overall growth rate is largest at $\alpha=1.0$. There is indeed a monotonic decrease in the value of the prefactor D as α decreases. In Fig. 9 we display the unnormalized data for $S(0,t)$ at $\alpha=1.0$, 0.5, 0.45, and 0.4. These lines are linear to a good degree of accuracy, and

TABLE I. Numerical least-squares fits to the expression $y-y_0=D(t-t_0)^{2n}$ using the peak of the structure function $S(0,t)$ to define a squared length for the kinetic Glauber ANNNI model. The values of $S(0,t)$ were normalized to a maximum value of 1. In some cases two different time regimes have been studied to check the consistency of the fits. The error Δ is based on the central limit theorem. MCS represents the Monte Carlo steps per site.

System size	k_BT_f/J_0	α	$\Delta t^{(1)}$/MCS	$10^{-4}\times D^{(1)}$	$2n^{(1)}$	$\Delta t^{(2)}$/MCS	$10^{-4}\times D^{(2)}$	$2n^{(2)}$	$\pm\Delta$
128×128	0.2	1.0	30–400	6.41	1.00	60–400	6.41	1.00	0.05
60×120	0.2	0.8	20–200	2.35	1.0				0.1
140×140	0.2	0.8	40–200	2.90	1.06				0.05
128×128	0.2	0.55	60–200	3.33	1.05	120–400	4.07	1.02	0.05
140×140	0.2	0.5	40–200	2.31	0.97				0.05
128×128	0.2	0.45	30–300	0.654	1.09	120–600	0.869	1.05	0.05
128×128	0.2	0.4	60–600	0.275	1.05				0.05
128×128	1.0	0.5	20–400	1.52	0.94	200–400	1.31	0.95	0.05
128×140	0.2	0.35	500–3400	0.066	1.0				0.1
140×140	1.9	0.9	40–200	3.09	0.96				0.05

also the drop in growth rate is evident. An interesting feature of this variation of the growth rate is that it does not seem to vary linearly with α, but the value of D decreases more steeply near the wetting line as it is approached from the dry region.

Table II shows the results of numerical fitting to the effective domain areas $A_i(t)$. Again, independent of α, the previous result $2n\simeq 1.0$ is recovered for both the x and y directions. Thus the anisotropy in the system manifests itself through the prefactors D_x and D_y, but leaves the dynamical exponent intact. In the dry region the growth rate is larger in the x direction than in the y direction. At $\alpha=1.0$, the ratio D_x/D_y is largest, and has the value of about 3.5. When α decreases the ratio also decreases to about 1.4 just before the wetting line. Immediately in the wet region the ratio becomes less than one, as the domain configurations in Fig. 6 indicate. As α is reduced further, the domain growth becomes extremely anisotropic due to the appearance of superheavy-light clusters in the x direction. Indeed, at $\alpha=0.35$ the growth rate in the y direction is about 500 times faster than in the x direction. Despite this the dynamical exponents remain the same.

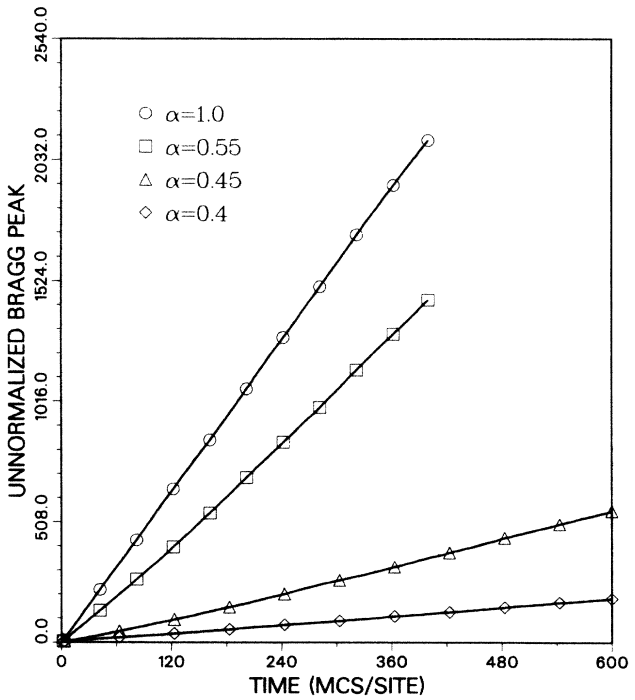

FIG. 9. The time development of the peak of the anisotropic structure function $S(0,t)$ as a function of the anisotropy parameter α. All results are for 128^2 systems at $k_BT_f/J_0=0.2$. There is an overall slowing-down effect in the growth rate as α decreases and also a more abrupt change near $\alpha=0.5$. However, the dynamical exponents remain the same, as indicated by the straightness of these lines.

The last two entries in Tables I and II yield the results of numerical fits at high temperatures. In both cases there is an overall reduction in the growth rate. However, within the accuracy of our results there is also a reduction in the value of the dynamical exponent. In the case of the effective domain areas this may be an indication of the breakdown of the approximation $A_i(\infty)=0$. However, the results for $S(0,t)$ also indicate this change in n, although $S(0,t)$ should be less sensitive to changes in temperature.

C. Structure functions and dynamical scaling

The anisotropic growth mode manifests itself not only through the prefactors D_x and D_y but also in the shape of the structure function $S(\mathbf{k},t)$. This can be made quantitative by defining *generalized directional moments* in the (k_x,k_y) plane as[15,16]

$$k_m(\theta,t)\equiv \sum_{k=0}^{k_c} k(\theta)^m S(k(\theta),t) \Big/ \sum_{k=0}^{k_c} S(k(\theta),t)\ , \qquad (12)$$

where θ is the angle between $k(\theta)$ and the k_x direction and k_c is an ultraviolet cutoff parameter. Thus $\theta=0$ and $\theta=\pi/2$ correspond to the mth moments in the x and y directions, respectively. Using this definition the scaling ansatz can also be generalized to include anisotropy, as we will discuss below.

To study the nature of the anisotropic structure function we have computed $S_1(\mathbf{k},t)$ in the plane $k_x,k_y\geq 0$ both in the dry and wet regions. In Figs. 10(a) and 10(b)

TABLE II. Power-law fits to (10) using the normalized inverse squared perimeter lengths $A_i(t)$ $(i=x,y)$ to define effective domain areas in the x and y directions. Note the excellent agreement with the dynamical exponents of Table I. The ratios of the prefactors D_x and D_y have also been computed to obtain quantitative information about the axial anisotropy of the growth. Error is the same as in Table I.

System size	k_BT_f/J_0	α	$\Delta t^{(1)}$/MCS	$D_x^{(1)}$ $D_y^{(1)}$	$2n_x^{(1)}$ $2n_y^{(1)}$	$\Delta t^{(2)}$/MCS	$D_x^{(2)}$ $D_y^{(2)}$	$2n_x^{(2)}$ $2n_y^{(2)}$	$D_x^{(1)}/D_y^{(1)}$ $D_x^{(2)}/D_y^{(2)}$	$\pm\Delta$
128×128	0.2	1.0	30–200	12.45 3.56	1.01 0.99				3.50	0.05
60×120	0.2	0.8	20–200	7.29 3.51	0.99 0.98				2.08	0.06
140×140	0.2	0.8	40–200	5.90 3.37	1.03 1.00				1.75	0.05
128×128	0.2	0.55	60–200	5.30 2.85	0.98 0.98	120–400	4.60 3.42	1.01 1.01	1.38 1.35	0.05
140×140	0.2	0.5	40–200	2.06 4.41	0.94 1.05				0.47	0.05
128×128	0.2	0.45	30–300	0.66 2.38	0.91 1.11	120–600(x) 120–300(y)	0.42 3.26	0.98 1.07	0.28 0.13	0.05
128×128	0.2	0.4	30–300(x) 30–200(y)	0.85 1.31	0.97 1.06				0.80	0.05
140×140	0.2	0.35	50–200	0.003 1.56	1.09 0.83	150–200	0.005 0.57	1.01 0.98	0.002 0.009	0.05
128×140	0.2	0.35	1000–4000	4.94×10^{-3}	1.0	50–1500	0.33	0.1	1.5×10^{-3}	0.1
128×128	1.0	0.5	20–400	1.80 3.84	0.82 0.78	200–400	0.71 1.17	0.94 0.94	0.45 0.61	0.05
140×140	1.9	0.9	40–200	5.40 0.77	0.79 0.71	100–200	2.57 0.26	0.89 0.86	6.97 9.96	0.05

we depict $S(\mathbf{k},t)$ along the directions k_x and k_y as a function of time for a 120×60 system at $\alpha=0.8$, $k_BT_f/J_0=0.2$. The structure function is narrowest in the x direction, consistent with the anisotropic growth mode. We have also computed the inverses of the generalized second moments for the directions $k_x=0$, $k_y=0$, $2k_x=k_y$, together with a circularly averaged total second moment. Although these quantities also define $\bar{R}^{\,2}(t)$, we have not used them for determining the growth exponent due to their dependence on k_c.

The corresponding results for $S(\mathbf{k},t)$ in the case of a 128×128 system in the wet region at $\alpha=0.4$, $k_BT_f/J_0=0.2$ are similar to Fig. 10, except that in this case the structure function is narrowest in the y direction, since a change in the anisotropic growth mode has occurred. For a finite system $S(k_x,k_y=0,t)$ remains very broad for a long time due to the presence of a large number of domain walls in the x direction.

To test the anisotropic scaling we have calculated scaling functions with several definitions of the length scale. First, using the generalized second moments, a scaling function

$$F(x)=k_2(\theta,t)S(k(\theta),t)\ ,\qquad x=k(\theta)/[k_2(\theta,t)]^{1/2} \tag{13}$$

can be defined. This function is also going to depend somewhat on the direction θ. Second, we have also calculated the scaling function

$$\tilde{F}(\tilde{x})=S(k(\theta),t)/S(0,t)\ ,\qquad \tilde{x}=k(\theta)[S(0,t)]^{1/2}\ . \tag{14}$$

In some cases we also tested scaling using definitions of length involving $A_i(t)$. In the dry region scaling was found to hold to a very good degree of accuracy with all these definitions for the case $\alpha=0.8$, $k_BT_f/J_0=0.2$. Thus, all length scales studied are essentially equivalent. In Figs. 11(a)–11(c) we show some of the scaling functions calculated in this case. In Figs. 12(a)–12(c), scaling results are depicted in the wet region for the structure function calculated at $\alpha=0.4$, $k_BT_f/J_0=0.2$. Again, scaling was found to hold to a good degree of accuracy. However, due to the broadness of the peak in the x direction scaling was not as good along the k_x axis as in other directions, as Fig. 12(c) indicates. In this case it obviously takes a longer time to reach the true asymptotic scaling regime than in the dry region.

III. PHENOMENOLOGICAL THEORY OF DOMAIN GROWTH IN THE ANNNI MODEL

The characteristic feature of the kinetic ANNNI Glauber model at low temperatures is that a simple power growth law seems to be valid to a very good de-

gree of accuracy. Also, the growth exponents estimated from various definitions of a length have values very close to $n=\frac{1}{2}$, almost independent of the anisotropy parameter α. This suggests very strongly that there exists an underlying universal growth mechanism in this model which governs the growth law at late times. Indeed, the domain configurations encountered during growth (see Figs. 3, 6, and 8) suggest that there are two main ingredients in the growth process of the kinetic ANNNI model. First, the reduction in curvature of domain walls is clearly visible as a function of time. This feature is typical of the Allen-Cahn mechanism,[4-6] where the motion of the interfaces is diffusively driven by the curvature. In the well-known $p=2$ nonconserved case with a scalar order parameter and a double-well potential, it has been shown by several authors[4-6] that a $t^{1/2}$ growth law follows from this mechanism. In the case of the ANNNI model we can write the time-dependent Langevin equation as[2,3]

$$\partial\Psi/\partial t=-\underline{L}\,\delta H/\delta\Psi+\xi(\mathbf{r},t)\ , \tag{15}$$

where H is the Landau-Ginzburg-Wilson (LGW) Hamiltonian[30] of the model, ξ is a random noise term, and $\underline{L}$ is the kinetic matrix. The order parameter $\Psi=(\psi_1\psi_2)^T$ is now a two-component quantity so that the equations of motion for ψ_1 and ψ_2 are of the form

$$\begin{aligned}\partial\psi_1/\partial t&=-L_{11}\,\delta H/\delta\psi_1-L_{12}\,\delta H/\delta\psi_2+\xi\ ,\\ \partial\psi_2/\partial t&=-L_{21}\,\delta H/\delta\psi_1-L_{22}\,\delta H/\delta\psi_2+\xi\ ,\end{aligned} \tag{16}$$

where the L_{ij} are matrix elements of $\underline{L}$. The explicit coupling of ψ_1 and ψ_2 makes it nontrivial to generalize the standard Allen-Cahn derivation for the case of a two-component order parameter. However, along any direction of the order parameter space (where $\psi_1\propto\psi_2$), this derivation can be formally done. Thus, if we imagine performing an "averaging" over all of the (ψ_1,ψ_2) space, the $t^{1/2}$ growth law may remain unchanged. Due to the high degeneracy of the ground state there are restrictions on the possible domain configurations in the system. In particular, there is a large number of *vertices* present during the growth (see Figs. 3, 6, and 8). This was already pointed out in an earlier study of the model.[15] The presence of these vertices sets restrictions on the motion of the interfaces since the latter are coupled to these defects. Indeed, the Monte Carlo configurations suggest that an argument of the Allen-Cahn type is not sufficient to obtain the universal growth mechanism because the vertices are present even at late times. To include the constraints due to the vertices, we consider a theory due to Kawasaki,[11,12] who has derived equations of motions for a different system, the p-state clock model ($p\geq 3$) which is similar to our system in that the interfaces and vertices are coupled. These equations have been derived from the general Langevin equation (14) using the idea of virtual displacements. Indeed, the existence of vertices for the p-state clock models has been demonstrated in computer simulations.[17] Analogous four-rayed vertices are encountered in the ANNNI model during the domain growth as well. There are also three-rayed vertices but for simplicity we shall omit them here. If we assume the validity of these equations for the kinetic ANNNI model (which is reasonable given the similarities of the topologies during domain growth between these two models) we can write them as

$$\partial\phi/\partial t=L(\nabla^2-\hat{\mathbf{n}}\hat{\mathbf{n}}:\nabla\nabla)\phi\ , \tag{17a}$$

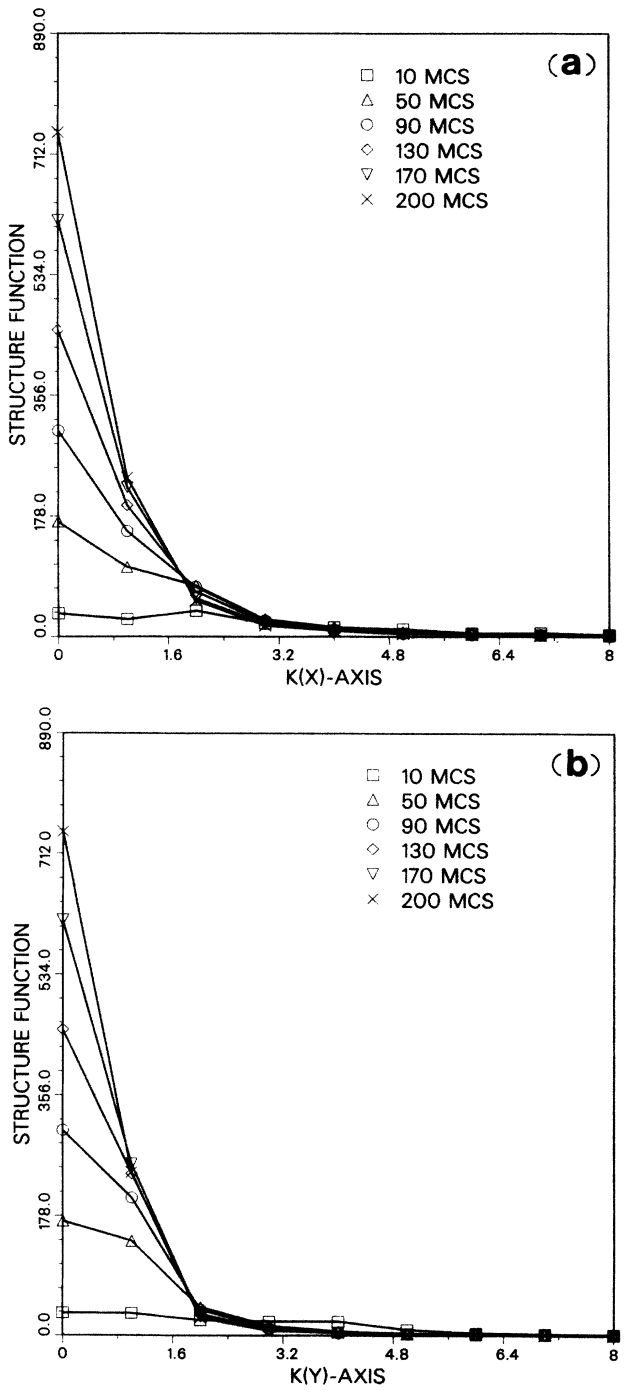

FIG. 10. Time development of the anisotropic structure function $S(\mathbf{k},t)$ for a 120×60 system in the dry region at $\alpha=0.8$, $k_BT_f/J_0=0.2$: (a) $S(k_x,k_y=0,t)$ and (b) $S(k_y,k_x=0,t)$. This function is about a factor of 2 narrower in the x direction than in the y direction, which reflects the anisotropic growth mode.

$$L^{-1}\underline{\epsilon}(\tau,t)\cdot\partial\mathbf{q}(\tau,t)/\partial t=\sum_{j=1}^{4}\sigma_j(\hat{\mathbf{n}}_j\times\hat{\tau})\ , \tag{17b}$$

for four-rayed vertices of the type shown in Fig. 13(a). The first equation is written for a phase variable ϕ which is singular along the interfaces, with $\hat{\mathbf{n}}\equiv\nabla\phi/|\nabla\phi|$. The second equation describes explicitly the motion of four-rayed vertices, where $\mathbf{q}$ denotes the position of the *defect line* where four interfaces forming the vertex meet, and $\hat{\tau}$ is the unit vector parametrizing this line. Again, L is the kinetic coefficient, σ_j is the anisotropic surface tension, and $\underline{\epsilon}$ denotes the mass density tensor

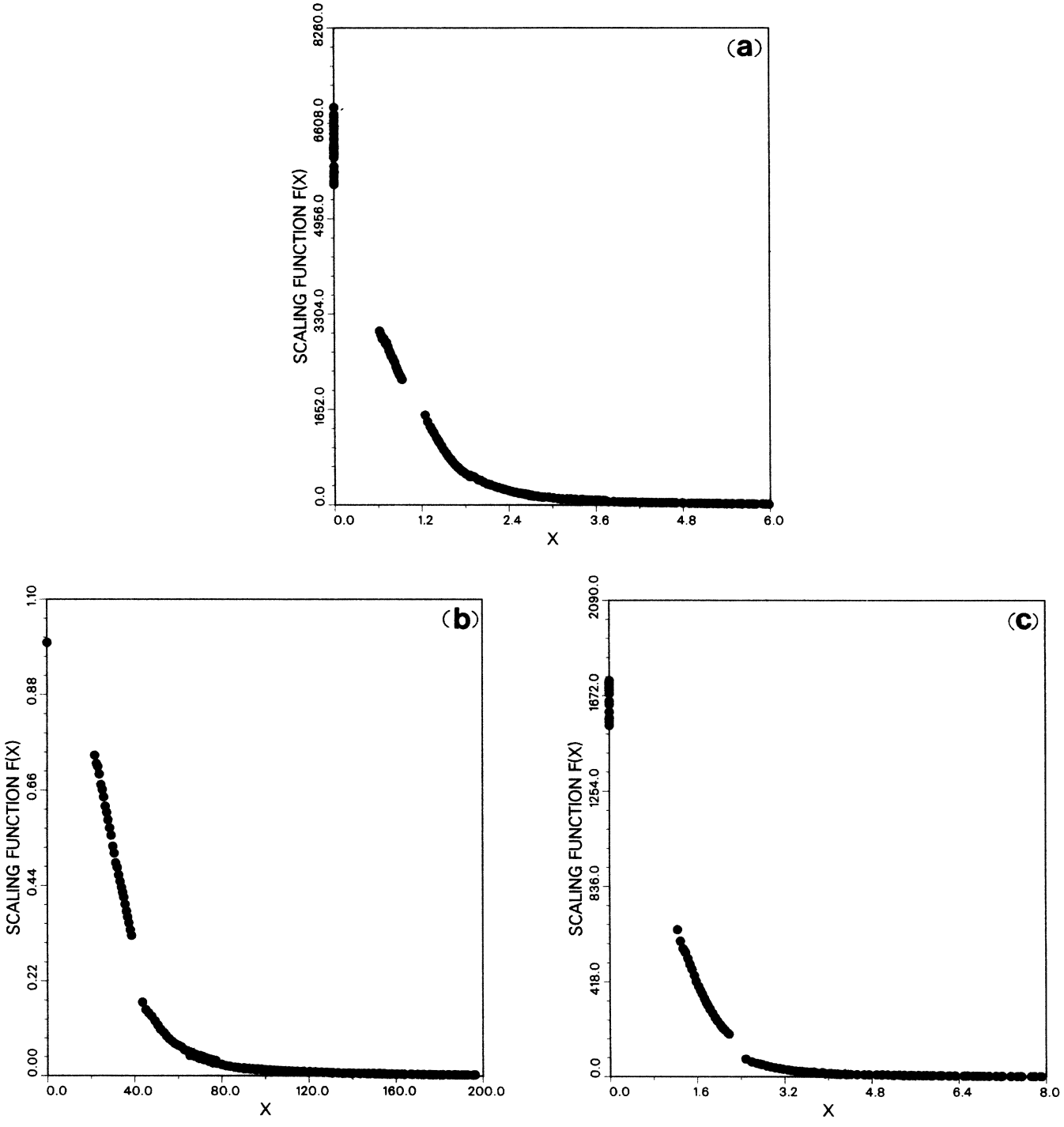

FIG. 11. Scaling functions of the structure factor in the dry region for a 120×60 system at $\alpha=0.8$, $k_BT_f/J_0=0.2$. (a) Scaling with the generalized second moment $k_2^{(x)}$ $(k_y=0,t)$ along the k_x axis, (b) scaling with the peak of the structure factor $S(0,t)$ along the k_y axis, and (c) scaling along the line $2k_x=k_y$ with the corresponding generalized second moment $k_2^{(xy)}$ $(2k_x=k_y,t)$. In all cases studied the scaling was found to hold to a very good degree of accuracy independent of the definition of length used.

associated with the defect line. (We have also subsumed the anisotropy of L in $\underline{\epsilon}$.) The right-hand side of (17b) can be considered to be the net surface tension force acting on the defect tube, while the left-hand side is the friction force due to the motion of the defect tube. Using (17) and averaging over anisotropies, Kawasaki[12] has shown that the problem can be reduced to the dissipative dynamics of opposite "Coulomb charges" from which a $t^{1/2}$ growth law follows both in $d=2$ and $d=3$ using dimensional arguments. This result is consistent with our simulations and the value $n=0.5$ which we have obtained.

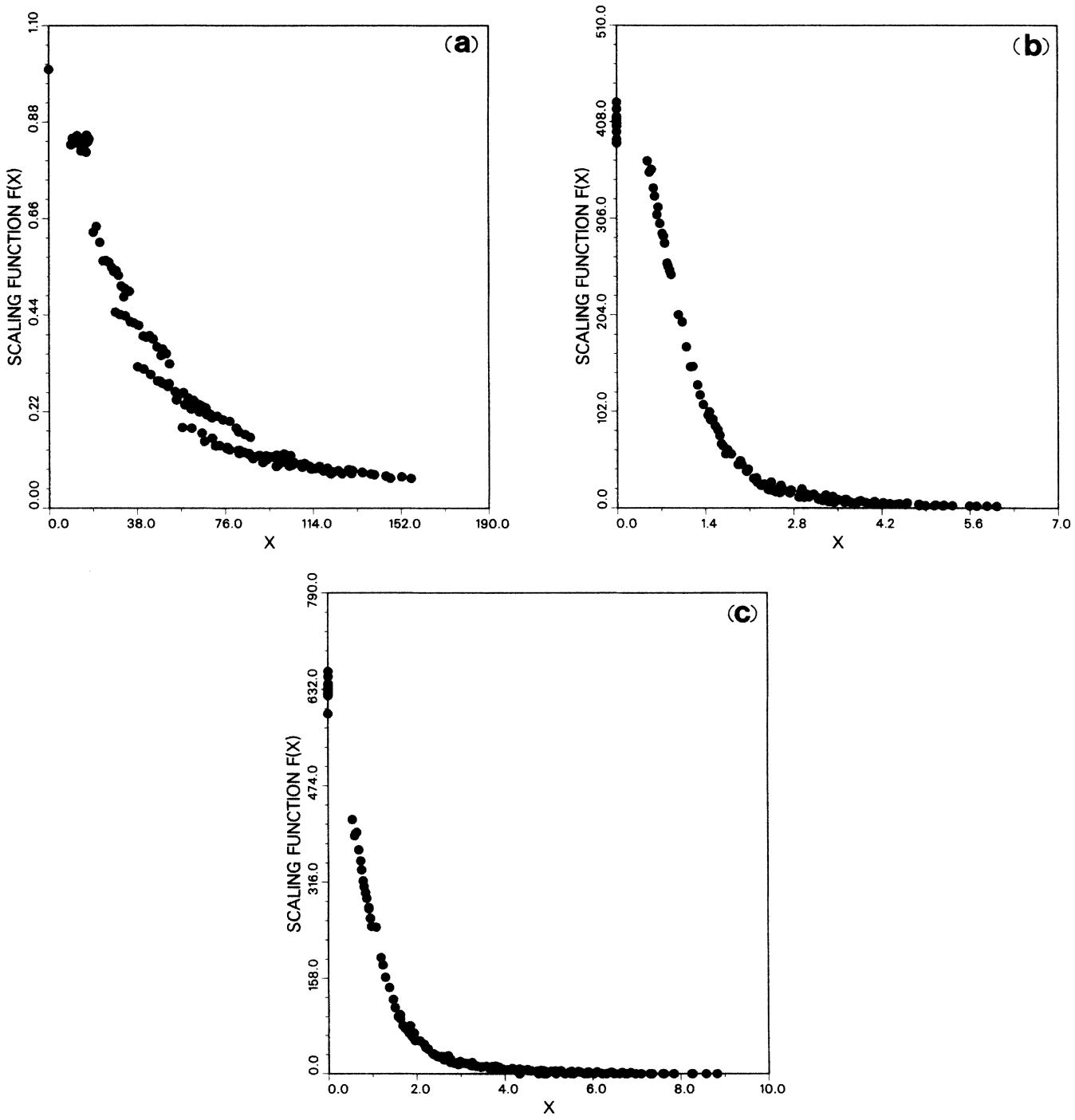

FIG. 12. Dynamical scaling functions of the wet structure function computed at $\alpha=0.4$, $k_B T_f/J_0=0.2$ for a 128^2 system. (a) Scaling along the k_x axis with the peak of the structure function $S(0,t)$, (b) scaling along the k_y axis with the generalized second moment $k_2^{(y)}$ $(k_x=0,t)$, and (c) scaling along the line $k_x=k_y$ with the corresponding second partial moment $k_2^{(xy)}$ $(k_x=k_y,t)$. A slower growth in the wet region makes it more difficult to reach the asymptotic scaling regime, which is evident from (a).

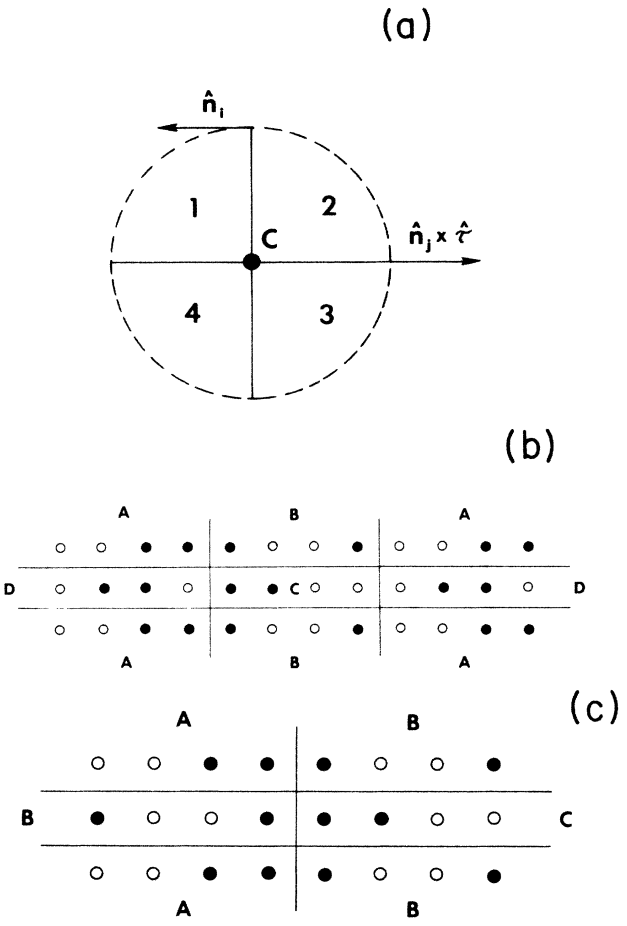

FIG. 13. (a) A schematic four-rayed vertex. Dashed circle encloses the tube core C from which four interfaces separating the four degenerate ground states 1, 2, 3, and 4 emerge. (b) A dominant vertex-antivertex configuration in the ANNNI model shown here in a quadrupole configuration. There are two vertex-antivertex pairs consisting of a heavy $(A \mid B)$, light $(C \mid D)$, soft superheavy $(D \mid C)$, and soft superlight $(C \mid D)$ walls. The energies of the vertex interfaces are $0.5J_0$ and $0.5\alpha J_0$ in the y and x directions, respectively. After the wetting transition this configuration becomes unfavorable due to the instability of the soft superheavy-light walls. (c) A vertex configuration consisting of (wet) heavy-light walls only. Three-rayed vertices consisting of combinations of heavy-light and superheavy-light walls are also possible.

Equations (17) neglect thermal noise. In Kawasaki's original derivation there were two additional terms present in (17b). Namely, there is a contribution arising from the finite radius of the vertex core C in Fig. 13(a), which may in most cases be safely neglected. More importantly, Kawasaki's derivation also included a term arising from the misfit parameter δ in the *chiral* clock model.[20] This term vanishes for the ordinary clock model. However, for the ANNNI model a similar term should be present, because the anisotropy parameter α plays a role analogous to δ, with $\delta \sim (1-\alpha)$. Thus this term is identically zero only at the decoupling point $\alpha = 1$, where there is an exact energetic degeneracy between the relevant walls in the model (as mentioned before). It is then easy to see intuitively from (16) how the anisotropy arises in the ANNNI model. Namely, even at $\alpha = 1$ the microscopic structures of the domain walls in the x and y directions are different. Thus, the coupled equations of motion arising from (17) are expected to reflect this anisotropy. In addition to this, as $\alpha < 1$ the uniaxial chirality $(1-\alpha)$ along x axis couples to the equations of motion and changes the anisotropy.

We conclude this section by noting that a more quantitative version of the above argument can be made,[31] based on a decoupling approximation for (17b). This leads to an Allen-Cahn–type growth law in both the x and y directions. In addition, predictions are obtained for the ratio of the amplitudes D_x/D_y of these growth laws which are in reasonable agreement with the Monte Carlo results shown in Table II. The interested reader is referred to Ref. 31 for more details.

IV. SUMMARY AND DISCUSSION

In this paper we have performed an extensive Monte Carlo study of the anisotropic growth of the (2.2) antiphase in the two-dimensional ANNNI model, and, in particular, determined quantitatively the effect of the wetting transition on the domain growth. To explain the results obtained we have proposed that a phenomenological theory based on the existence of vertex-antivertex pairs is relevant for the model and leads to a universal $t^{1/2}$ behavior. Also, we have estimated the anisotropy from this theory and obtained a good agreement between this estimate and the Monte Carlo results. In particular, we have been able to explain the rather sudden change in the anisotropic growth mode as one crosses the wetting line by invoking an argument based on an alteration in the vertex mechanism as one of the relevant walls becomes unstable.

As we have mentioned in the introduction, the previous results obtained for the ANNNI model with conserved (Kawasaki) dynamics suggest[16] that an exponent $n \simeq 0.5$ is obtained in the limit of large systems and long times. Our new simulations at $\alpha = 1$ also support this result. This suggests that the vertex-interface mechanism is valid for this case as well, which raised an interesting question about the role of uniaxiality in possible dynamical universality classes. Namely, in contrast to our results, in a study of the nearest-neighbor–next-nearest-neighbor (NN-NNN) Ising model which has a symmetric $p = 4$ phase Sadiq and Binder[13] (SB) suggested a universal exponent $n = \frac{1}{3}$ associated with a long-range diffusion process with conserved dynamics. This model has no vertex-antivertex formation and thus $n = \frac{1}{2}$ may become impossible. A similar conclusion seems to apply to the (3×1) phase in a model of H/Fe(110) studies by Vinãls and Gunton,[32] who obtained an effective exponent $n \simeq 0.14$–0.25 with conserved dynamics. However, with *nonconserved* dynamics SB obtained the result $n = \frac{1}{2}$. This is actually not a trivial result due to the high degen-

eracy of the ground state but may indicate the dominant role of curvature in such a two-component order parameter system, as we have briefly discussed in Sec. III. The role of uniaxiality is also supported by our new results on the domain growth in a model of O/Pd(110), which has a uniaxial (3×1) phase.[14] In this case, an exponent $n\simeq0.5$ is again obtained for both Glauber and Kawasaki dynamics. This system has a natural vertex-antivertex formation with three-rayed vertices, similar to the three-state clock model.

Finally, we want to speculate about the nature of the scaling functions for the ANNNI model. Namely, it would be of great interest to generalize the derivation of the nonconserved Ising scaling function[6,7] to include a spatially anisotropic domain distribution. This derivation together with a careful Monte Carlo study would be needed to further clarify the nature of the dynamical universality classes for the uniaxial Ising models. This work is currently underway.

ACKNOWLEDGMENTS

We want to thank Professor Martin Grant for many patient discussions. This work is supported by National Science Foundation (NSF) Grant No. DMR-86-12609 and U.S. Office of Naval Research (ONR) Grant No. N00014-83-K-0382. One of us (T.A.-N.) is also supported by the Academy of Finland and the Neste Corporation of Finland.

[1]K. Binder, in *Condensed Matter Research Using Neutrons,* edited by S. W. Lovesy and R. Scherm (New York, Plenum, 1985), p. 1.

[2]J. D. Gunton and M. Droz, *Introduction to the Theory of Metastable and Unstable States,* Vol. 183 of *Lecture Notes in Physics,* edited by H. Araki, J. Ehlers, K. Hepp, R. Kippenhahn, H. A. Weidenmüller, and J. Zittartz (Springer-Verlag, Berlin, 1983).

[3]J. D. Gunton, M. San Miguel, and P. S. Sahni, *The Dynamics of First Order Phase Transitions* in *Phase Transitions and Critical Phenomena,* edited by C. Domb and J. L. Lebowitz (Academic, London, 1983), Vol. 8; J. D. Gunton, J. Stat. Phys. **34**, 1019 (1984); K. Binder, *Condensed Matter Research Using Neutrons, Today and Tomorrow, Lecture Notes for NATO* (Plenum, New York, 1985).

[4]I. M. Lifshitz, Zh. Eksp. Teor. Fiz. **42**, 1354 (1962) [Sov. Phys.—JETP **15**, 939 (1962)].

[5]S. M. Allen and J. W. Cahn, Acta Metall. **27**, 1085 (1979).

[6]K. Kawasaki, M. C. Yalabik, and J. D. Gunton, Phys. Rev. A **17**, 455 (1978).

[7]T. Ohta, D. Jasnow, and K. Kawasaki, Phys. Rev. Lett. **49**, 1223 (1982).

[8]G. F. Mazenko and O. T. Valls, Phys. Rev. B **27**, 6811 (1983); **30**, 6732 (1984); F. C. Zhang, O. T. Valls, and G. F. Mazenko, *ibid.* **31**, 1529 (1985); S. R. Anderson, G. F. Mazenko, and O. T. Valls, J. Stat. Phys. **41**, 17 (1985).

[9]C. Kawabata and K. Kawasaki, Phys. Lett. **65A**, 137 (1978); M. K. Phani, J. L. Lebowitz, M. H. Kalos, and O. Penrose, Phys. Rev. Lett. **45**, 366 (1980); P. S. Sahni, G. Dee, J. D. Gunton, M. K. Phani, J. L. Lebowitz, and M. H. Kalos, Phys. Rev. B **24**, 410 (1981); K. Kaski, M. C. Yalabik, J. D. Gunton, and P. S. Sahni, *ibid.* **28**, 5263 (1983); J. Viñals, M. Grant, M. San Miguel, J. D. Gunton, and E. T. Gawlinski, Phys. Rev. Lett. **54**, 1264 (1985); E. T. Gawlinski, S. Kumar, M. Grant, J. D. Gunton, and K. Kaski, Phys. Rev. B **32**, 1575 (1985).

[10]E. T. Gawlinski, M. Grant, J. D. Gunton, and K. Kaski, Phys. Rev. B **31**, 281 (1985).

[11]K. Kawasaki, Ann. Phys. (N.Y.) **154**, 319 (1984).

[12]K. Kawasaki, Phys. Rev. A **31**, 3880 (1985).

[13]A. Sadiq and K. Binder, Phys. Rev. Lett. **51**, 674 (1983); A. Sadiq and K. Binder, J. Stat. Phys. **35**, 517 (1984).

[14]T. Ala-Nissila and J. D. Gunton, in *Kinetics of Interface Reactions,* edited by H. J. Kreuzer and M. Grunze (Springer-Verlag, Berlin, 1987); T. Ala-Nissila and J. D. Gunton (unpublished).

[15]K. Kaski, T. Ala-Nissila, and J. D. Gunton, Phys. Rev. B **31**, 310 (1985).

[16]T. Ala-Nissila, J. D. Gunton, and K. Kaski, Phys. Rev. B **33**, 7583 (1986).

[17]K. Kaski and J. D. Gunton, Phys. Rev. B **28**, 5371 (1983); G. S. Grest and D. J. Srolovitz, *ibid.* **30**, 6535 (1984); K. Kaski, M. Grant, and J. D. Gunton, *ibid.* **31**, 3040 (1985).

[18]P. S. Sahni, G. S. Grest, M. P. Anderson, and D. J. Srolovitz, Phys. Rev. Lett. **50**, 263 (1983); P. S. Sahni, D. J. Srolovitz, G. S. Grest, M. P. Anderson, and S. A. Safran, Phys. Rev. B **28**, 2705 (1983); G. S. Grest and P. S. Sahni, *ibid.* **30**, 226 (1984); G. S. Grest, D. J. Srolovitz, and M. P. Anderson, Phys. Rev. Lett. **52**, 1321 (1984); K. Kaski, J. Nieminen, and J. D. Gunton, Phys. Rev. B **31**, 2998 (1985).

[19]W. Selke and W. Pesch, Z. Phys. B **47**, 335 (1982); D. A. Huse, A. M. Szpilka, and M. E. Fisher, Physica **121A**, 363 (1983); M. E. Fisher, J. Stat. Phys. **34**, 667 (1984); I. Sega, W. Selke, and K. Binder, Surf. Sci. **154**, 331 (1985).

[20]D. A. Huse and M. E. Fisher, Phys. Rev. B **29**, 239 (1984).

[21]P. Rujan, G. V. Uimin, and W. Selke, Phys. Rev. B **32**, 7453 (1985).

[22]T. Ala-Nissila, J. Amar, and J. D. Gunton, J. Phys. A **19**, L41 (1986).

[23]P. Rujan, W. Selke, and G. Uimin, Z. Phys. B **65**, 235 (1986).

[24]W. Selke and M. E. Fisher, Z. Phys. B **40**, 71 (1980); W. Selke, *ibid.* **43**, 335 (1981).

[25]J. Kroemer and W. Pesch, J. Phys. A **15**, L25 (1982).

[26]M. N. Barber, J. Phys. A **15**, 915 (1982).

[27]J. Villain and P. Bak, J. Phys. (Paris) **42**, 657 (1982); M. N. Barber and P. M. Duxbury, J. Phys. A **14**, L251 (1981); P. M. Duxbury and M. N. Barber, *ibid.* **15**, 3219 (1982); M. N. Barber and P. Duxbury, J. Stat. Phys. **29**, 427 (1982); P. D. Beale, P. M. Duxbury, and J. Yeomans, Phys. Rev. B **31**, 7166 (1985); A. Finel and D. de Fontaine, J. Stat. Phys. **43**, 645 (1986).

[28]G. Ertl and J. Küppers, Surf. Sci. **21**, 61 (1970); P. Rujan, W. Selke, and G. Uimin, Z. Phys. B **53**, 221 (1983); P. Rujan and G. V. Uimin, J. Phys. A **17**, L61 (1984).

[29]A. Milchev, D. W. Heermann, and K. Binder, Z. Phys. B **63**, 521 (1986).

[30]A. Z. Patashinskii and V. L. Pokrovskii, *Fluctuation Theory of Phase Transitions* (Pergamon Press, London, 1979).

[31]T. Ala-Nissila, Ph.D thesis, Temple University, 1986.

[32]J. Viñals and J. D. Gunton, Surf. Sci. **157**, 473 (1985).